

Characterization of copper added tellurium-rich chalcogenide thin films

Pramesh Chandra¹, Arvind K. Verma², R. K. Shukla³
and Anchal Srivastava⁴

^{1,2,3,4} Department of Physics, University of Lucknow, Lucknow, U.P. – 226007, India

Abstract

The present study reports characterization studies of tellurium-rich chalcogenide thin films $\text{Te}_{90-x}\text{Se}_{10}\text{Cu}_x$ with varying proportions of copper from zero to twenty through ten. The films have been deposited by thermal evaporation method. Bulk samples used for preparation of thin films were synthesized using melt quenching technique. XRD spectra show polycrystalline structure for all the films with reorientation of Te atoms along different planes as copper content is varied. Surface morphology shows uniform distribution of nano-sized grains in all cases but the grain size gradually reduces as copper content increases. Absorption is quite low in the near infrared region whereas transmission is zero in the ultra violet and visible regions. Interference maxima-minima are observed in the near infrared range and the film with 10% copper content shows highest transmission percentage. Photoluminescence spectra studied at two different excitation wavelengths – 380 nm and 430 nm – show green emission which is spread in different ranges of the visible spectrum. For a particular excitation wavelength, emission occurs at the same wavelength for all the films. The intensity varies and is found to be highest for 20% copper content and lowest for 10% copper content.

Keywords: XRD, FESEM, Near infrared (NIR), Transmission, Photoluminescence

1. Introduction

Chalcogenides are a very important class of materials due to their varied technological applications in switching and memory devices, xerography, phase change recording, etc. [1-4]. These materials are used for development of active and passive infrared devices. These are low-phonon energy materials and are generally transparent from the visible to infrared region [5, 6].

Among the chalcogen family, selenium (Se) and tellurium (Te) have been studied widely due to their potential applications. These are promising materials having tremendous utility in solar cells, optical limiting, filters, IR emitters, optical rewritable data, IR detectors, antireflection coatings, gratings, optical

recording media, etc. [7-10]. Chalcogenide glasses have flexible structure and each atom can adjust its neighbouring environment so that the valance requirements are satisfied. The interest in these materials arises due to their ease of fabrication in the form of both bulk as well as thin films. Se-Te alloys have more advantages than pure chalcogens due to their greater hardness, higher crystallization temperature, higher photosensitivity and smaller ageing effects [11, 12]. Moreover, the physical properties of these alloys depend on their compositions. Addition of a third element like Cu, Bi, Sb, Sn, Pb, Cd, Hg etc. in Se-Te binary alloy is expected to change the properties of the host alloy and behave as a chemical modifier. This produces noticeable changes in the properties of chalcogenides.

Tellurium-rich alloys attracted a lot of attention due to their potential applications. Researchers have reported that tellurium-rich alloys offer good transparency in the infrared region thereby making these glasses a good choice for optical devices [13, 14]. Tellurium-rich glassy alloys of Se-Te are widely used for commercial, scientific, and technological purposes. Their application ranges from optical recording media to xerography [15, 16].

The present work intends to study the effects of addition of copper on the structural, morphological and optical properties of tellurium rich chalcogenide thin films $\text{Te}_{90-x}\text{Se}_{10}\text{Cu}_x$ ($x = 0, 10, 20$).

2. Materials and Methods

2.1 Synthesis

Melt quenching technique was used to synthesize the three samples – $\text{Te}_{90}\text{Se}_{10}$, $\text{Te}_{80}\text{Se}_{10}\text{Cu}_{10}$ and $\text{Te}_{70}\text{Se}_{10}\text{Cu}_{20}$ – in bulk form. 5N pure component materials purchased from Sigma Aldrich were weighed in proportion of their respective atomic

weight percentages as per requirements of the samples. These were put in different quartz ampoules each of length 6 cm and internal diameter 8 mm. Vacuum $\sim 10^{-4}$ Torr was created by a rotary pump for evacuating the ampoules. During the process of evacuation itself, the ampoules were sealed thermally with the help of oxygen–Liquefied Petroleum Gas (LPG) flame torch. The sealed ampoules were then kept in a muffle furnace. Heating was done at the rate of $4^{\circ}\text{C}/\text{min}$ upto 1000°C and this temperature was maintained for 10 hours. The ampoules were frequently rocked during heating so as to ensure proper homogenization of the melt. After 10 hours, the red hot ampoules were taken out from the furnace and quenched in ice-cold water. The quenched samples were recovered by breaking the quartz ampoules. The solid samples were then crushed and filtered with filter cloth. The process was followed repeatedly till the bulk samples were obtained in the form of fine powder.

Thermal evaporation method was used for depositing the thin films on well-cleaned glass substrates. HINDHIVAC coating unit Model No. 12A4D was used and bulk samples were kept in a molybdenum boat. Vacuum $\sim 4 \times 10^{-6}$ mbar was maintained inside the bell jar. The rate of deposition was continuously measured by a quartz crystal monitor Hindhivac DTM-101. Films of thickness 221 nm, 283 nm and 173 nm were synthesized for $\text{Te}_{90}\text{Se}_{10}$, $\text{Te}_{80}\text{Se}_{10}\text{Cu}_{10}$ and $\text{Te}_{70}\text{Se}_{10}\text{Cu}_{20}$ respectively.

Before depositing the thin films, the glass substrates were chemically cleaned. Commercially available glass slides from Blue Star, Mumbai, India were dipped in chromic acid for six hours. After washing with liquid detergent, the slides were finally cleaned in acetone in an ultrasonic cleaner.

2.2 Characterization

The films were characterized by X-ray diffraction (XRD), Field Emission Scanning Electron Microscopy (FESEM), UV-Visible-NIR spectroscopy and Photoluminescence (PL) spectroscopy. XRD studies were done at a scanning rate of $2^{\circ}/\text{min}$ employing Cu K_{α} radiation wavelength 1.54056 \AA by Ultima IV diffractometer from Rigaku, Japan. FESEM images of the films were taken using JSM-7610F model from JEOL, Japan. Before taking the images, gold-palladium coating was done on the films using JEC-3000FC auto fine coater from JEOL, Japan. Optical absorption and transmission spectra were recorded using Jasco V670 UV-Vis-NIR spectrophotometer and Photoluminescence (PL) spectra were recorded with the help of LS55 Perkin Elmer Fluorescence spectrometer. All the measurements were performed at room temperature.

3. Results and Discussion

3.1 X-ray diffraction (XRD) studies

X-ray diffraction patterns of the $\text{Te}_{90-x}\text{Se}_{10}\text{Cu}_x$ ($x = 0, 10, 20$) thin films are shown in figure 1. All the films show polycrystalline structure. For $\text{Te}_{90}\text{Se}_{10}$ film i.e. at $x = 0$, prominent peaks are observed at angular positions 23.07° , 27.82° and 40.57° which have orientations along (100), (101) and (110) planes respectively corresponding to tellurium [17]. Most intense peak is the one which is along (100) plane. When copper (Cu) is used as an additive in the form of $\text{Te}_{80}\text{Se}_{10}\text{Cu}_{10}$ thin film, the XRD pattern shows peaks at angular positions 23.06° , 27.62° and 40.51° . Planes corresponding to these angular positions are the same, as discussed for $\text{Te}_{90}\text{Se}_{10}$. Slight shifting towards lower values is observed as compared to those found in $\text{Te}_{90}\text{Se}_{10}$. All these peaks correspond to Te as seen earlier [17]. In this case, the most intense peak is found to be along (101) plane instead of (100) plane, as in case of $\text{Te}_{90}\text{Se}_{10}$. The intensity corresponding to (101) plane is also greater than that observed for $\text{Te}_{90}\text{Se}_{10}$ along the same plane.

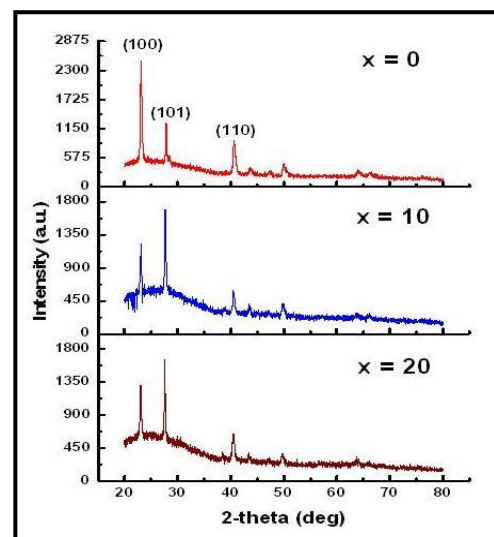


Figure 1: XRD spectra of $\text{Te}_{90-x}\text{Se}_{10}\text{Cu}_x$ ($x = 0, 10, 20$) thin films

As 20% copper is added replacing tellurium by the same amount, XRD pattern of $\text{Te}_{70}\text{Se}_{10}\text{Cu}_{20}$ film shows prominent peaks at 22.99° , 27.57° and 40.51° . These are at slightly shifted angular positions, of lower values, as compared to those seen in case of $\text{Te}_{90}\text{Se}_{10}$. From [17], it can again be said that all these peaks correspond to Te along (100), (101) and (110) planes respectively. In this case, the most intense peak is again observed to be along (101) plane instead of (100) plane, as was found in $\text{Te}_{90}\text{Se}_{10}$. The intensity corresponding to (101) plane is also greater

than the one found along same plane for $\text{Te}_{90}\text{Se}_{10}$. The crystallite size along these planes, as shown in table 1, was determined by Scherrer formula [18],

$$d = K \lambda / \beta \cdot \cos \theta \quad (1)$$

where d is average crystallite size, $K = 0.9$, $\lambda_{\text{Cu-K}\alpha} = 1.54056 \text{ \AA}$, β - FWHM in radians, θ - Bragg angle.

Table 1: Crystallite size along different planes for $\text{Te}_{90-x}\text{Se}_{10}\text{Cu}_x$ ($x = 0, 10, 20$) thin films

$\text{Te}_{90-x}\text{Se}_{10}\text{Cu}_x$ samples	Crystallite size along different planes (nm)		
	(100)	(101)	(110)
$x = 0$	25.1	49.4	17.6
$x = 10$	34.1	38.0	19.4
$x = 20$	28.9	44.7	18.4

With gradual increase in the percentage of copper from zero to twenty through ten, it has, in general, been observed that there is slight shifting, although of different values, in angular positions of the peaks of tellurium. This indicates reorientation of tellurium atoms in different planes, which is reflected in varying intensities of the XRD peaks. The peaks corresponding to the metal additive do not appear at all. Processes such as heat treatment at different temperatures, laser/solar irradiation etc. [19-21] may be of great utility for increasing intensities of the already obtained peaks. According to requirement, peaks may also be manipulated/controlled using these processes with optimum proportion of metal additive. Further work along these lines is being pursued.

3.2 Surface morphological studies

Figure 2 (a), (b) and (c) show the FESEM images of $\text{Te}_{90-x}\text{Se}_{10}\text{Cu}_x$ thin films for $x = 0, 10$ and 20 respectively. All the films reveal nano size of grains. For $x = 0$, the grains are equal in size and spherical in shape. These are uniformly distributed over the entire surface. The size of the grains is $\sim 30 \text{ nm}$. When copper (Cu) is added in $\text{Te}_{90}\text{Se}_{10}$ to form $\text{Te}_{80}\text{Se}_{10}\text{Cu}_{10}$, the grains are found to be distributed uniformly in a compact manner like the cells of a beehive. The grains are unequal in size and are mostly pentagonal in shape. Average grain size is $\sim 20 \text{ nm}$.

For $x = 20$, the grains are again found to be distributed uniformly over the surface with average size $\sim 12\text{-}15 \text{ nm}$. It is, therefore, observed that the grain size is getting reduced with increasing copper content.

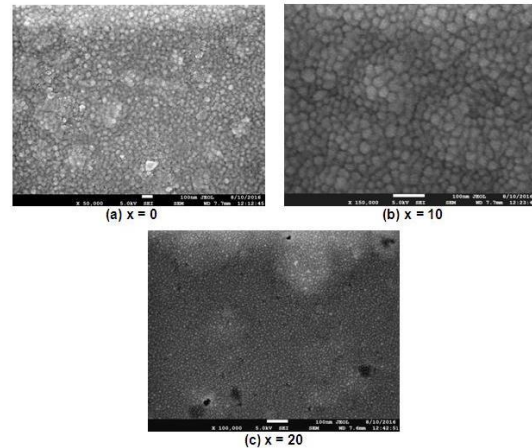


Figure 2: FESEM images of $\text{Te}_{90-x}\text{Se}_{10}\text{Cu}_x$ thin films for (a) $x = 0$, (b) $x = 10$ and (c) $x = 20$

3.3 Optical absorption spectra

Absorption spectra recorded in the near infrared (NIR) spectral range $1000 - 2700 \text{ nm}$ for the three $\text{Te}_{90-x}\text{Se}_{10}\text{Cu}_x$ ($x = 0, 10, 20$) thin films are shown in figure 3. It is clear that the film without addition of copper i.e. $x = 0$ shows comparatively higher absorption upto 1500 nm in the reported range. All the films show low absorption in the spectral range $1500 - 2700 \text{ nm}$. The film with 10% copper content shows least absorption in $1900 - 2700 \text{ nm}$ range.

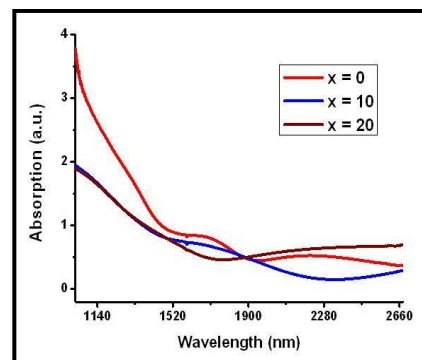


Figure 3: Absorption spectra of $\text{Te}_{90-x}\text{Se}_{10}\text{Cu}_x$ ($x = 0, 10, 20$) thin films

3.4 Optical transmission spectra

Figure 4 shows transmission spectra of $\text{Te}_{90-x}\text{Se}_{10}\text{Cu}_x$ ($x = 0, 10, 20$) thin films in $250 - 2700 \text{ nm}$ range which is from ultra violet (UV) to near infrared (NIR) region through the visible spectrum. It is seen that all the three films have zero transmission in the UV and visible regions. This trend continues in the

infrared region as well and insignificant transmission is observed up to 1500 nm.

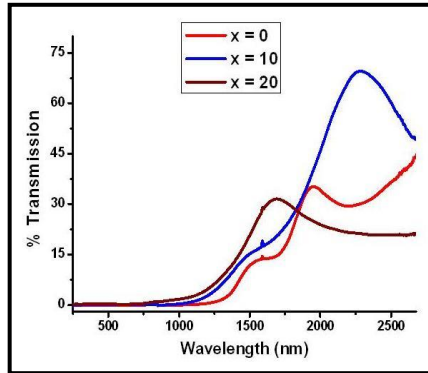


Figure 4: Transmission spectra of $\text{Te}_{90-x}\text{Se}_{10}\text{Cu}_x$ ($x = 0, 10, 20$) thin films

As the wavelength is further increased, maxima and minima are seen in the transmission spectra of all the films, which is indicative of homogeneity of the deposited films [22]. This is due to interference of the reflected wave fronts from the two surfaces of the film. The patterns indicate thin good quality films. The film having 10% copper content shows the highest transmission maxima of 70% at 2287 nm whereas the other two films show transmission maxima which are less than 40%. These films can thus have applications in infrared optics with desirable transmission in the different ranges.

3.5 Photoluminescence (PL) spectroscopy

PL spectrum is an indication of the different energy states existing between the valence and conduction bands [23]. Figure 5 (a) and (b) show PL spectra for the three thin films at two different excitation wavelengths (λ_{ex}) 380 nm and 430 nm respectively. For $\lambda_{\text{ex}} = 380$ nm, emission is found to occur in green region at same wavelength 515 nm (2.40 eV) for all the films. PL intensity, however, varies and is found to be highest for the film having 20% copper content, whereas lowest intensity is observed for the film with 10% copper content.

As excitation wavelength is changed to 430 nm, emission is found to occur again in the green region. The peculiar point is that each film now shows emission at two distinct wavelengths – 530 nm (2.33 eV) and 569 nm (2.17 eV) – in contrast to that seen for 380 nm excitation wavelength, where only one emission peak was observed for each film. In this case, too, the two emission peaks are the same for all the three thin films. Out of the two PL emission peaks, the ones occurring for all the films at 530 nm have much lower intensities as compared to the ones

occurring at 569 nm. The order of PL intensities are the same as was observed for $\lambda_{\text{ex}} = 380$ nm.

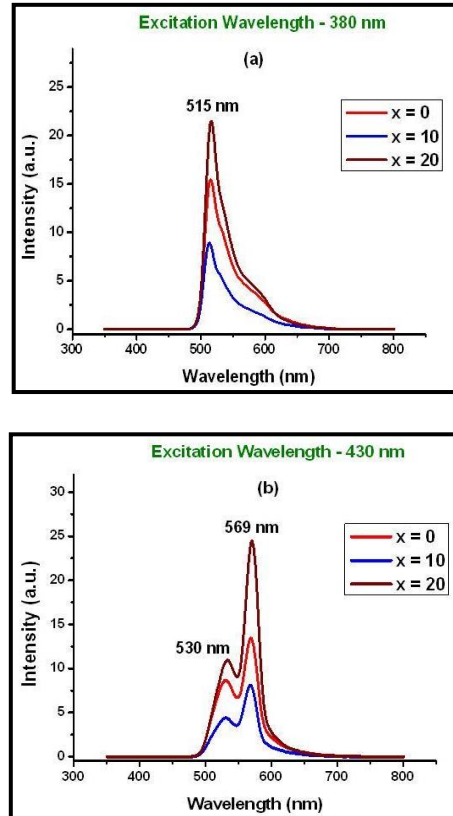


Figure 5: PL spectra of $\text{Te}_{90-x}\text{Se}_{10}\text{Cu}_x$ ($x = 0, 10, 20$) thin films for (a) 380 nm and (b) 430 nm excitation wavelengths

4. Conclusions

$\text{Te}_{90-x}\text{Se}_{10}\text{Cu}_x$ ($x = 0, 10, 20$) thin films were deposited on glass substrates by thermal evaporation method. XRD patterns indicate that the films are polycrystalline. As copper content is varied, positions of peaks found for $x = 0$ slightly shift and reorientation of Te atoms is seen in varying intensities of planes. Peaks corresponding to the added metal do not develop at all. FESEM images show nano-sized and uniformly distributed grains for all the films. Gradual reduction in grain size is found with increasing copper content. Absorption is quite low in the NIR region whereas the films show zero transmission in the UV and visible regions. Transmission increases for all the films in the NIR region and the film with 10% copper content shows highest transmission. PL spectra show emission at same wavelength for all the films at a particular excitation wavelength. Emission is spread in the green region at both the excitation wavelengths for all the films. Films with 20% and 10% copper contents show highest and lowest PL intensities

respectively for both the excitation wavelengths. These thin films can be promising alternatives, as per requirements, for applications in electronics, infrared optics and optoelectronics.

Acknowledgments

Financial assistance from UGC, New Delhi vide project F. No. 42-773/2013(SR) is gratefully acknowledged. Authors are also thankful to Govt. of the state of Uttar Pradesh, India through Centre of Excellence Scheme for providing XRD facility at the Department of Physics, University of Lucknow.

References

- [1] Zakery A. and Elliott S. R., Optical properties and applications of chalcogenide glasses: a review, *Journal of Non-Crystalline Solids*, Vol 330 (Issue 1): 1 – 12, (2003).
- [2] Kumar A., Lal M., Sharma K., Tripathi S. K. and Goyal N., Meyer-Neldel rule and dc conduction in $\text{Se}_{85-x}\text{Te}_{15}\text{Ge}_x$ glasses, *Indian Journal of Pure and Applied Physics*, Vol 51 (Issue 4): 251 – 253, (2013).
- [3] Kumar A., Lal M., Sharma K., Tripathi S. K. and Goyal N., Electrical Properties of $\text{Se}_{85-x}\text{Te}_{15}\text{In}_x$, *Chalcogenide Letters*, Vol 9 (Issue 6): 275 – 285, (2012).
- [4] Al-Agel F. A., Al-Arfaj E. A., Al-Marzouki F. M., Khan S. A., Khan Z. H. and Al-Ghamdi A. A., Phase transformation kinetics and optical properties of Ga–Se–Sb phase-change thin films, *Materials Science in Semiconductor Processing*, Vol 16 (Issue 3): 884 – 892, (2013).
- [5] Savage J. A., *Infrared Optical Materials and their Antireflection Coatings*, Adam Hilger Ltd.: Bristol, (1985).
- [6] Sharma K., Lal M., Kumar A. and Goyal N., Photoelectrical Properties of Semiconducting Amorphous Se-Te-Sb Thin Films, *Journal of Ovonic Research*, Vol 10 (Issue 1): 7 – 13, (2014).
- [7] Khan Z. H., Al-Ghamdi A. A. and Al-Agel F. A., Crystallization kinetics in as-synthesis high yield of a- $\text{Se}_{100-x}\text{Te}_x$ nanorods, *Materials Chemistry and Physics*, Vol 134 (Issue 1): 260 – 265, (2012).
- [8] Khan Z. H., Glass transition kinetics of a- $\text{Se}_x\text{Te}_{100-x}$ nanoparticles, *Science of Advanced Materials*, Vol 4 (Issue 2): 232 – 238, (2012).
- [9] Chou J. C., Yang S. Y. and Wang Y. S., Study on the optoelectronic properties of amorphous selenium-based xerographic photoreceptors for electrophotography, *Materials Chemistry and Physics*, Vol 78 (Issue 3): 666 – 669, (2003).
- [10] Pawar S. M., Moholkar A.V., Rajpure K.Y. and Bhosale C. H., Photoelectrochemical investigations on electrochemically deposited CdSe and Fe-doped CdSe thin films, *Solar Energy Materials and Solar Cells*, Vol 92 (Issue 1): 45 – 49, (2008).
- [11] Shimakawa K., On the temperature dependence of a.c. conduction in chalcogenide glasses, *Philosophical Magazine B*, Vol 46 (Issue 2): 123 – 135, (1982).
- [12] Kasap S. O., Wagner T., Aiyah V., Krylouk O., Bekirov A. and Tichy L., Amorphous chalcogenide $\text{Se}_{1-x-y}\text{Te}_x\text{P}_y$ semiconducting alloys: thermal and mechanical properties, *Journal of Materials Science*, Vol 34 (Issue 15): 3779 – 3787, (1999).
- [13] Desevedavy F. et al., Te-As-Se glass microstructured optical fiber for the middle infrared, *Applied Optics*, Vol 48 (Issue 19): 3860 – 3865, (2009).
- [14] Michel K. et al., Development of a chalcogenide glass fiber device for in-situ pollutant detection, *Journal of Non-Crystalline Solids*, Vol 326: 434 – 438, (2003).
- [15] Ohta T., Phase-change optical memory promotes the DVD optical disk, *Journal of Optoelectronics and Advanced Materials*, Vol 3 (Issue 3): 609 – 626, (2001).
- [16] Ho N. et al., Single-mode low loss chalcogenide glass waveguides for the mid-infrared, *Optics Letters*, Vol 31 (Issue 12): 1860 – 1862, (2006).
- [17] Powder Diffraction Data File, Joint Committee of Powder Diffraction Standard, International Center for Diffraction Data, USA card no. 00-004-0554
- [18] Cullity B. D. and Stock S.R., *Element of X-ray diffraction*. Adison – Wesley Publishing Company, Vol 1: 531, (1956).
- [19] Ahmad S., Ganaie M., Khan M. S. and Zulfequar M., Effect of laser and visible light irradiation on structural and optical properties of thin films of amorphous selenium and selenium mercury (80:20 composition), *Advanced Materials Letters*, Vol 5 (Issue 9): 511 – 519, (2014).
- [20] Hafiz M. M., El-Kabany N., Kotb H. M. and Bakier Y. M., Annealing Effects on Structural and Optical Properties of $\text{Ge}_{10}\text{Sb}_{30}\text{Se}_{60}$ Thin Film, *International Journal of Thin Films Science and Technology*, Vol 4 (Issue 3): 163 – 171, (2015).
- [21] Alwany A. E. B., Algradee M. A., Hafith M. M. and Abdel-Rahim M. A., Effect of Heat Treatment on the Optical Properties of $\text{Ge}_{20}\text{Se}_{70}\text{Zn}_{10}$ Thin Films, *Academic Journal of Applied Sciences Research*, Vol 1 (Issue 1): 21 – 33, (2016).
- [22] Malik K., Parvinder, Gupta A. and Kumar P., Dispersive optical constants of thermally evaporated $\text{Se}_{70-x}\text{Te}_{30}\text{Pb}_x$ thin films, *Journal of Ovonic Research*, Vol 11 (Issue 2): 61 – 72, (2015).
- [23] Nogriya V., Dongre J. K., Ramrakhiani M. and Chandra B. P., Electro- and Photo-Luminescence Studies of CdS Nanocrystals prepared by organometallic precursor, *Chalcogenide Letters*, Vol 5 (Issue 12): 365 – 373, (2008).